Organic photoelectrochemical cells with quantitative photocarrier conversion

Antonio Guerrero,[1] Marta Haro,[1] Sebastiano Bellani,[2] Maria Rosa Antognazza,[2] Laura Meda,[3] Sixto Gimenez,*[1] Juan Bisquert*[1]

[1] Photovoltaics and Optoelectronic Devices Group, Departament de Fisica, Universitat Jaume I, 12071 Castello, Spain

[2] Center for Nano Science and Technology @Polimi, Istituto Italiano di Tecnologia, Via Pascoli 70/3, 20133 Milano, Italy

[3] ENI-Donegani Institute, Research Center for Non-Conventional Energies Via Fauser 4, 28100 Novara, Italy

Corresponding authors Email: sjulia@uji.es, bisquert@uji.es

30 September 2015

Abstract

Efficient solar-to-fuel conversion in a cost-effective way constitutes one of the major challenges to replace the current energetic model based on fossil resources and power the planet with sunlight. In order to achieve this objective, the integration of low-cost raw materials into simple devices is mandatory. Herein, we demonstrate that Organic PhotoElectrochemical Cells (OPEC) offer promising perspectives for the production of solar fuels. We show that the photogenerated carriers at the organic active layer can be quantitatively extracted to drive photoelectrochemical reactions at the interface with a liquid solution. By a careful choice of the selective contact and the redox couple in the liquid medium, we can tune the energetics of the system and activate either oxidative or

reductive chemistry at the semiconductor/solution interface by the desired photoelectochemical reactions. This control allows the design of OPEC systems for the production of different fuels. The design rules to drive the desired electrochemical reaction are provided based on a comprehensive study of the energetic aspects of the OPEC configuration. These devices can be considered as a low-cost, reliable alternative to convert solar energy into chemical energy and open promising new avenues for the production of solar fuels.

Converting the energy of solar photons into chemical bonds is termed solar fuel production. This is the purpose of photoelectrochemical cells (PEC) that aim to convert abundant compounds dissolved in liquid medium into a useful fuel by electrochemical reactions powered only by solar photons. Reduction of CO_2 by similar means is also of great interest for environmental purposes. The realization of a cost-effective device would bring a major step towards reliable renewable energy economy, but it has not been achieved yet. The seminal work of Fujishima and Honda[1] showed that high energy photons can be converted into electrons and holes in a stable semiconductor (TiO_2) to realize water oxidation, with a net production of hydrogen gas. Recently, the quest of semiconductors that fulfils properties of light absorption, charge separation, and adequate energy levels for realizing the required photoelectrochemical reactions in combination with suitable surface catalysts, has driven a great research effort[2]. However, so far the mainstream of research in materials and processes involves either metal oxide inorganic semiconductors such as TiO_2,[3] Fe_2O_3,[4] WO_3[5] and $BiVO_4$[6] or conventional photovoltaic materials as Si and $CuIn_{1-x}Ga_xSe_2$ (CIGS)[7].

Meanwhile, organic photovoltaic materials have experienced extraordinary development with a great potential to produce inexpensive devices. Organic bulk heterojunction (BHJ) operation is based on ultrafast transference of carriers from an absorbing polymer or small organic molecule to a functionalized fullerene[8]. Intermediate efficiency BHJ cells, such as the archetypal combination poly(3-hexylthiophene):[6,6]-phenyl C_{61}-butyric acid methyl ester (P3HT:PCBM) can provide up to ≈ 10 mA cm^{-2} photocurrent, 0.63 V open circuit voltage, and high fill factor using a standard configuration (Figure 1a). A careful combination of factors in the latest generation devices, such as optimization of donor-acceptor blend morphology, synthesis

of low bandgap molecules that show increased light absorption, and improvement of transport properties and selective contacts, has provided large efficiencies of solar to electricity conversion around 10%[9, 10]. The progress of organic cells demonstrates the versatility of organic photovoltaic materials, which can be designed and improved to realize highly efficient devices.

Despite these developments, the application of photoactive organic materials for solar fuel production has been very little explored. For the utilization of the BHJ blend materials in solar fuel production, two fundamental conditions must be met: (i) the organic blend must preserve the capability of generating charges even when it is in direct contact with a liquid electrolyte; (ii) the photovoltage must be high enough in order to allow efficient charge transfer between the organic film and the electrolyte. The coupling of photogeneration in organic conductors and blends with liquid electrolytes has been investigated for a long time,[11, 12, 13, 14, 15, 16] but the main electrochemical phenomena leading to gas evolution are still controversial. A detailed understanding of the interface processes is thus urgently needed, in order to fill the gap between the theoretically achievable photocurrent (on the base of conventional organic solar cells) and practical results obtained with PEC cells. [11, 17, 18, 19].

The PEC conversion requires the combination of two factors. The photovoltaic material in contact with a liquid medium must function efficiently in terms of charge absorption, internal charge separation, and transport to the active surface. The second step is that the interfacial charge transfer must occur at significant pace when the surface is contacted with the relevant compound to be transformed into a fuel, e.g., water or CO_2. This second aspect may require the assistance of a catalyst that facilitates the given electrochemical reaction. Unfortunately, up to date neither of both factors has been comprehensively studied in an Organic Photoelectrochemical Cell (OPEC)

configuration.

In summary, it is first necessary to demonstrate that the BHJ photovoltaic blend operates efficiently when the liquid medium replaces one of the metal contacts of the solar cell. In this paper we address this question and we show high current and voltage of standard P3HT:PCBM blends contacted by different electrolytes. We investigate the internal processes of photon-to-carrier conversion at the organic/liquid interface and we show inversion of current depending on the nature of contacts and redox couple. This study demonstrates the high potential of OPEC for solar fuel production.

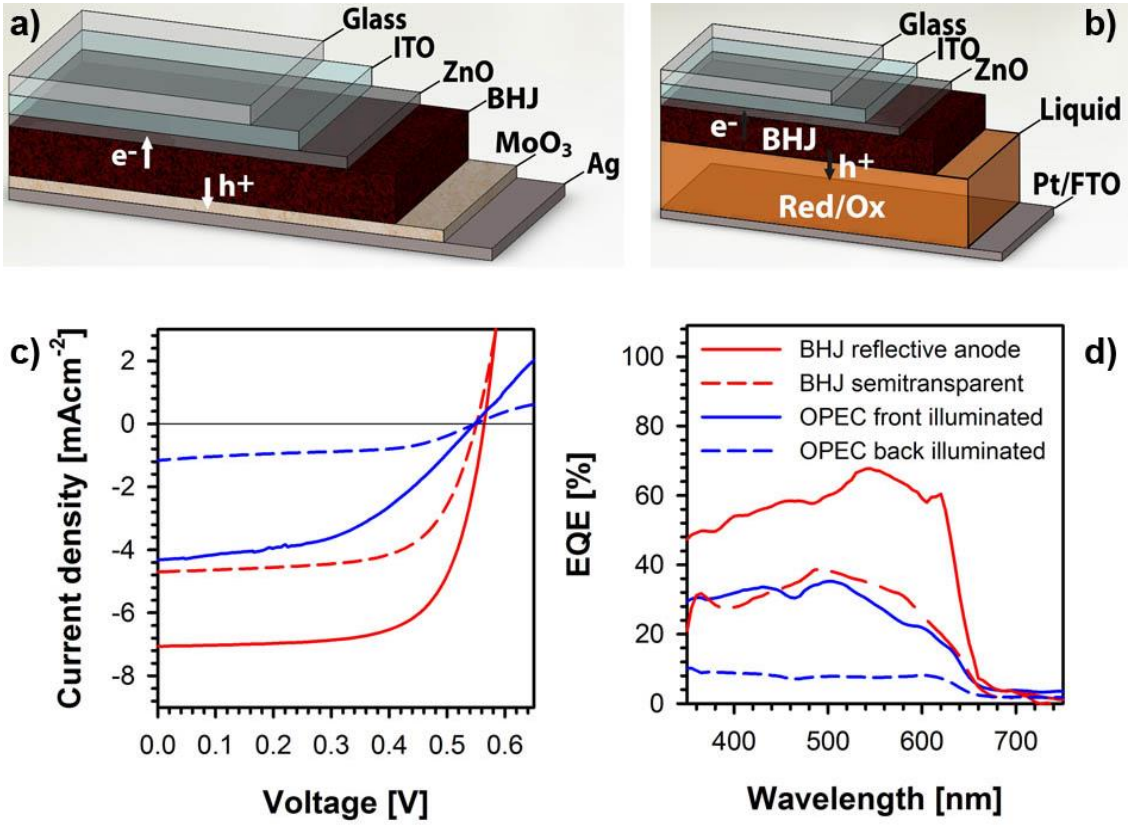

Figure 1: (a) Device architecture of a BHJ solar cell and (b) Organic Photoelectrochemical Cell (OPEC). The main difference in the OPEC configuration is the presence of a liquid solution with a redox couple able to extract carriers to the solution. (c) Current density/voltage characteristic and (d) External Quantum Efficiency (EQE) of devices fabricated in both configurations. Reflective and semi-transparent BHJ

refer to devices with 100 nm and 20 nm thick Ag layer, respectively.

Results and discussion

The first step in our study is to understand if there is a fundamental limitation in the photogeneration and charge extraction of carriers when a liquid electrolyte is in contact with the organic active layer. With this objective in mind, we prepared devices mimicking those known to work efficiently as BHJ solar cells (Figure 1a). In this configuration ZnO and MoO_3 act as interfacial layers (IFL) selective to electrons and holes, respectively. Fig. 1(c) shows the current density-voltage characteristics of representative organic BHJ solar cells with the structure ITO/ZnO/P3HT:PCBM/MoO_3/Ag. These cells show the standard electrical characteristics for this type of device widely reported in the literature.[20] When a thick layer of silver (100 nm) is used, the back contact acts as a mirror and reflects back some of the incident light, increasing the effective incident path length. On the other hand, when a thin layer of silver (20 nm) is used, the device is semitransparent and the light harvesting at the active layer is decreased, explaining the lower photocurrent observed. In the OPEC configuration the hole selective layer, MoO_3, was replaced by a redox couple able to accept holes from the active organic electrode in an organic solvent with a large electrochemical window (Figure 1b). In particular, an acetonitrile solution is used containing Ferrocene/Ferrocene$^+$ (Fc/Fc^+) as redox couple and tetrabutyl ammonium hexafluorophosphate ($N(Bu^n)_4PF_6$) as support electrolyte. When the MoO_3/Ag contact is replaced by the Fc/Fc^+ redox couple in the OPEC configuration with a Pt counterelectrode, a sizeable photocurrent of 4 mA cm^{-2} is observed, which is to the best of the authors' knowledge, the highest current reported in an all-organic PEC device. Interestingly, both semitransparent BHJ and OPEC show similar photoconversion properties as reflected by the external quantum efficiencies (EQE) in

Fig. 1(d). In addition, when the OPEC device is illuminated from the electrolyte, the photocurrent drops to about 1 mA/cm^2 due to the optical losses at the cell chamber. All these results clearly indicate that the OPEC device realizes quantitative carrier extraction to the electrolyte comparable to that of an optimized metal contact. An improvement of the optical engineering of the device may lead to enhanced photocurrents.

The rational design in an OPEC cell able to transform the incoming solar energy into chemical energy entails the adequate selection of the IFL and redox couple: this would allow efficient extraction of electrons or holes to the electrolyte solution through specific chemical reaction. For this purpose, two interfaces should be considered, both the IFL/organic blend and the organic blend/electrolyte interfaces. The first one has been intensively studied in organic photovoltaic devices since the energy level equilibration at the contacts determines the confinement of the electrical field providing efficient collection of carriers [21, 22, 23, 24]. Furthermore, regarding other kind of photoelectrochemical cells (based on colloidal quantum dots), it has been recently demonstrated that the selection of an adequate IFL can determine the sign of the photovoltage, i.e. the direction of the photogenerated charges (electrons and holes) that are driven to the collector and to the solution [25]. Taking all this into account, a hole (ZnO) and an electron (PEDOT:PSS) blocking layers have been selected as IFL in our OPEC devices. For the selection of the redox couples, Marcus theory [26, 27] has been considered and Fc/Fc^+ redox potential (4.9 eV) matches well with the HOMO level of the polymer (5.0 eV) and $BZQ/BZQ^{\cdot -}$ (with a redox potential 4.0 eV close to the LUMO of the fullerene, 3.2 eV). Consequently, both systems, Fc/Fc^+ and $BZQ/BZQ^{\cdot -}$ have been selected as hole and electron acceptors, respectively.

In order to elucidate whether the organic active layer is able to photogenerate similar

charge density in both PV and OPEC configurations, continuous-wave photoinduced absorption (CW-PIA) spectroscopy experiments were carried out. CW-PIA monitors the change in the transmission spectrum of the organic active layer due to the absorption of long-lived (>10μs) charged states. Hence, P3HT provides a spectroscopic fingerprint, which allows quantifying the occurrence of polarons in the presence of a redox electrolyte in contact with the organic blend. Figure 2 shows representative "in-phase" and "out-of-phase" CW-PIA spectra of the ITO/ZnO/BHJ and ITO/PEDOT:PSS/BHJ systems in air. The excited state photophysics of the P3HT/PCBM blend has been extensively studied in air, allowing the identification of the broad absorption feature between 620-1100 nm as due to two overlapping polaron absorption bands, peaking at 780 nm (free polarons) and at 960 nm (localized polarons) [28]. Figure 2 shows that, when the electrode ITO/ZnO/BHJ is immersed into an electrolyte solution containing the Fc/Fc^{+} redox couple, the polaronic fingerprint of P3HT matches the signal obtained in air, suggesting that charge generation within the organic BHJ is not altered by the presence of the liquid electrolyte. Similar results have been previously obtained in PPV-based polymers in contact with aqueous electrolytes, focusing however on much shorter timescales, relevant for charge generation processes [29]. On the other hand, when the ITO/PEDOT:PSS/BHJ system is immersed into the $BZQ/BZQ^{\cdot -}$ solution, the broad signal in the in-phase spectrum increases compared to that obtained in air and a clear response is observed in the out-of-phase spectrum (assigned to the absorption of very long-lived species). These two differences suggest longer photogenerated carrier lifetimes and can be ascribed to the presence of surface states that could slow down recombination [30, 31]. However, other causes that can increase the lifetime of the photogenerated charges cannot be excluded: as photoactivated doping that leads to more hydrophilic surfaces that changes the electrostatic interactions or screening of the

electric field probably due to a different orientation of the chains[32].

CW-PIA measurements of the systems immersed into the electrolyte solutions were repeated after 20 minutes, with identical results, indicating that no degradation phenomena affecting the photogeneration of charges in the organic blend take place within this time scale. All in all, these results suggest that the presence of a liquid electrolyte containing a redox couple does not significantly affect the photogeneration process in the active layer BHJ, increasing the polaron lifetime when BZQ/$BZQ^{\cdot-}$ acts as an electron scavenger.

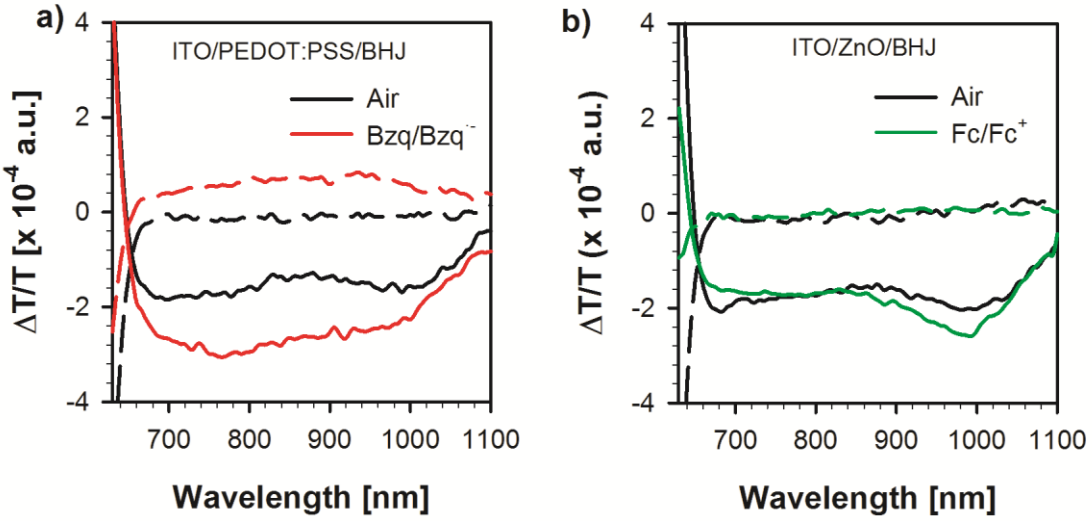

Figure 2: Continuous-wave photo-induced absorption spectra of (a) ITO/PEDOT:PSS/BHJ and (b) ITO/ZnO/BHJ in air and in the presence of BZQ-$BZQ^{\cdot-}$ and Fc-Fc^{+} redox couples, respectively. Solid lines correspond to in-phase response and dashed lines to out-of-phase response. Optical excitation at 561 nm, modulation frequency of 133 Hz.

The energetic aspects of the OPEC system have been studied using a three-electrode configuration, with Ag/Ag^{+} reference electrode, a graphite rod as counter-electrode and the system under study as working electrode. Figure 3 shows the *j-V* plots under chopped illumination for the designed systems to inject holes and electrons to the

solution, ITO/ZnO/BHJ/Fc-Fc^+ and ITO/PEDOT:PSS/BHJ/BZQ-$BZQ^{\cdot-}$, respectively (additional ITO/IFL/redox couple combinations are shown and discussed in the Supplemetary Information, Supplementary Figure S1). Figure 3a shows that the hole photocurrent (positive photocurrent) increases at positive bias indicating holes injected to the solution upon illumination and nearly 4 mA/cm^2 are achieved at +1V vs Fc-Fc^+. Moreover, the dark current is low indicating that the electrolyte and redox couple efficiently block the injection of electrons into the solution. Interestingly, at voltages close to –1V vs Fc-Fc^+ we observe an inversion of the photocurrent, indicating that electrons are collected by the solution. This inflexion point is related to the flatband potential V_{fb}, that designates the applied potential required to unfold the band. Similarly, figure 3b shows the increase of the electronic photocurrent (negative photocurrent) in the cathodic sweep indicating the injection of electrons from the system ITO/PEDOT:PSS/BHJ to the BZQ-$BZQ^{\cdot-}$ redox couple with practically zero dark current and an turn-on voltage of the photocurrent related to the position of V_{fb}. Again, the obtained photocurrent density is in the order of mA·cm^{-2}. These results demonstrate that the desired charge carriers can be injected into the electrolyte solution with an adequate selection of both IFL and redox couple.

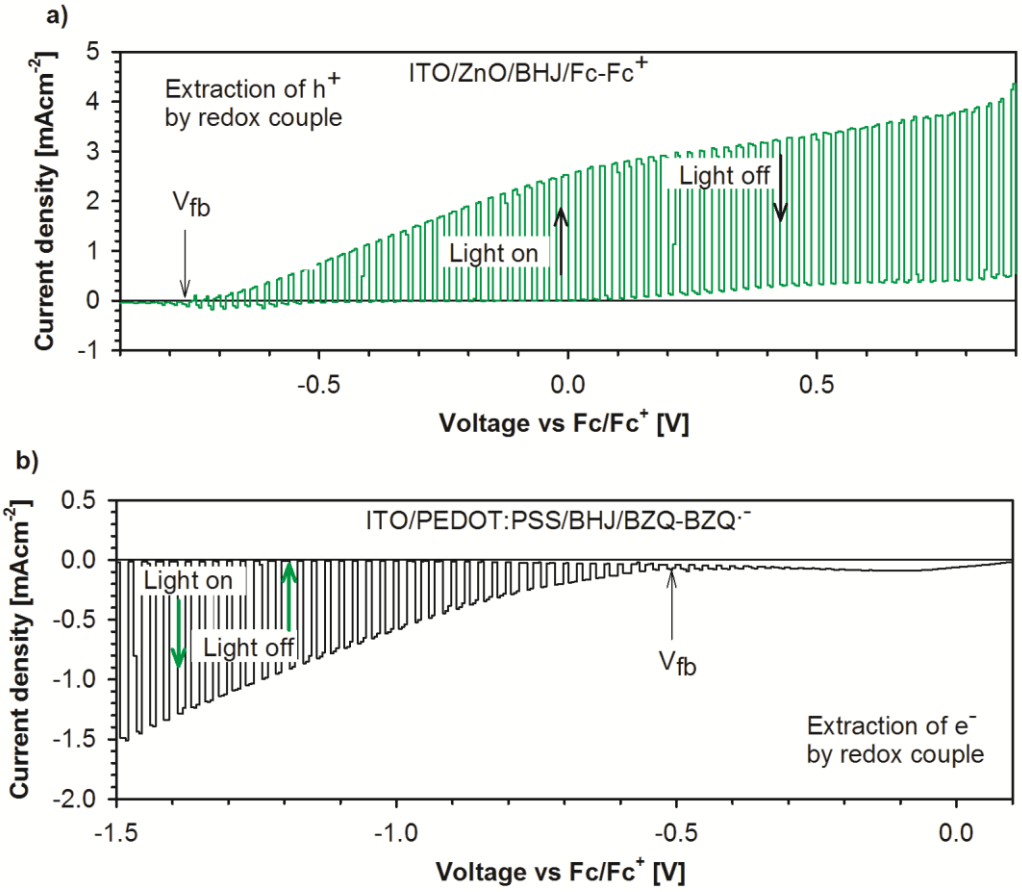

Figure 3: Shuttered J-V curves in acetonitrile (0.1M tetrabutyl hexafluorophosphate) recorded at 5 mV s^{-1} for ITO/PEDOT:PSS/BHJ/Fc-Fc^+ (a) and ITO/ZnO/BHJ/BZQ-$BZQ^{\cdot -}$ (b). The flatband potential (V_{fb}) extracted from Mott-Schottky analysis (see Figure 4) is also indicated.

In order to further understand the carrier dynamics of the devices, we performed capacitance-voltage measurements in three-electrode configuration. In this experiment, the working electrode is driven at a DC voltage and a small AC perturbation (1 kHz) is applied, the differential current output is measured and the capacitance is extracted. Representative Capacitance-Voltage measurements under dark conditions for two OPEC configurations are shown in Figure 4. These results are similar to those typically observed in OPVs: a constant capacitance that increases at intermediate applied voltages and equilibrates towards positive values. This behaviour is generally observed for p-

doped systems and has been previously correlated with the presence of a depleted layer at the organic layer/cathode interface [33]. From the Mott-Schottky analysis (C^{-2} versus V) the doping density (*n*) of the active layer can be extracted. The results for a selection of device configurations are shown as Table 1. Values of *n* are within the same order of magnitude to those previously observed in regular OPVs (n = 1-10 x10^{16} cm^{-3}) indicating that the presence of the liquid solution does not substantially modify the presence of electrically active impurities in the BHJ layer. Note that a different behaviour was observed in contact with aqueous saline electrolytes. [34] Although the doping density is related to the properties of the polymer itself, the obtained values are moderately increased by the use of a nano-sized porous ZnO layer that seems to restrict the domain size of the P3HT increasing the values of *n* [35]. In addition, doping values are uncorrelated with the redox couple used during the measurement.

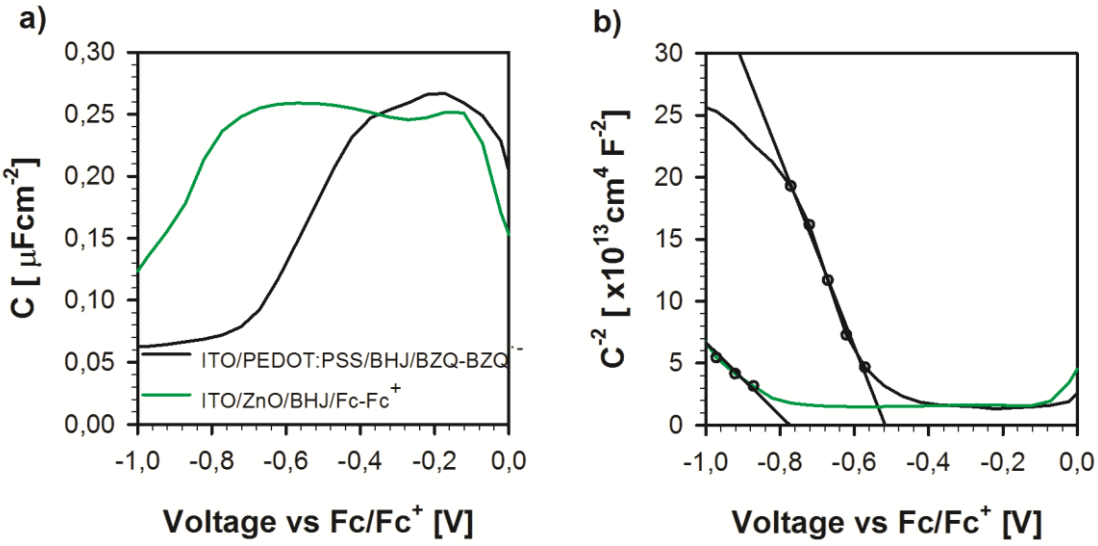

Fig. 4 Capacitance-Voltage response (a) and Mott-Schottky analysis (b) of ITO/PEDOT:PSS/BHJ in the presence of BZQ-$BZQ^{\cdot-}$ redox couple and ITO/ZnO/BHJ in contact with Fc-Fc^{+} redox couple.

On the other hand, the intercepts of the straight line with the x-axis are the values of V_{fb} collected in Table 1. At this applied voltage, bands will be flat and collection of

carriers at the contacts will not be favoured as carriers will only reach the contacts by diffusion. This explains the very low photocurrent values close to V_{fb} in Figure 3.

Table 1: Summary of doping density (*n*) and flat band potential (V_{fb}) extracted from Capacitance-Voltage data for selected OPEC configurations.

IFL	**Redox couple**	***n* [x 10^{16} cm^{-3}]**	**V_{fb} [V vs Fc/Fc^+]**
ZnO	$Fc\text{-}Fc^+$	16.0	-0.771
PEDOT:PSS	$Fc\text{-}Fc^+$	5.4	-0.490
PEDOT:PSS	$BZQ\text{-}BZQ^{\cdot-}$	6.17	-0.516
ZnO	$BZQ\text{-}BZQ^{\cdot-}$	38.0	-0.871

Figure 5 depicts the basic elements of the energetic landscape of both optimized OPEC devices (ZnO/BHJ/$Fc\text{-}Fc^+$ and PEDOT:PSS/BHJ/$BZQ\text{-}BZQ^{\cdot-}$), showing first the energy levels of the separate materials at constant vacuum level, on top, and the equilibrated junctions at flat Fermi level, on the bottom. The values for the work function of the $Fc\text{-}Fc^+$ and $BZQ\text{-}BZQ^{\cdot-}$ redox couples have been obtained by cyclic voltammetry and those for the organic blend, ZnO and PEDOT:PSS have been extracted from literature [23, 36, 37]. In these diagrams, we have considered a slightly doped organic semiconductor material ($n \sim 10^{16}\ cm^{-3}$), no surface states and a concentration of the redox couple high enough (>0.1 M) to consider that the potential drop fully takes place within the semiconductor material at the BHJ/solution interface [38]. Figures 5(c) and (d) clearly show that the energy levels of the system ITO/ZnO/BHJ/$Fc\text{-}Fc^+$ are well-aligned to drive the photogenerated electrons to the ZnO contact and the holes to the redox couple in the liquid phase. We believe that in these conditions the semiconductor is working under accumulation (the Fermi level intercepts the maximum of the valence band). On the other hand, the system ITO/PEDOT:PSS/BHJ/$BZQ\text{-}BZQ^{\cdot-}$ can drive the

photogenerated electrons to the electrolyte solution and the holes to the IFL. These schemes are in good agreement with the photoelectrochemical behavior showed in Figure 3.

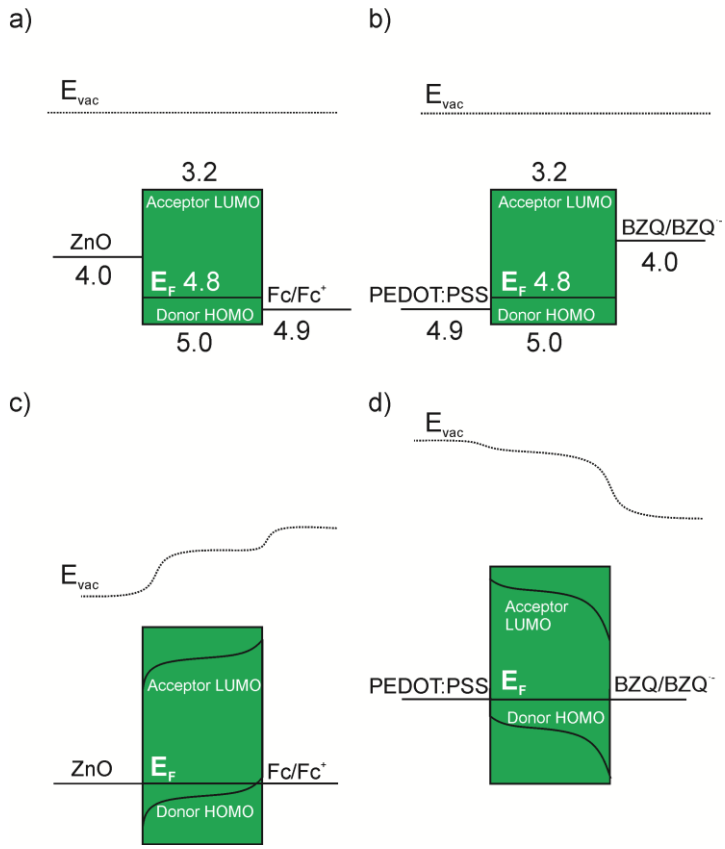

Figure 5. Energy level diagrams representing both high performing OPEC configurations before and after electrical equilibration. The vacuum level is also included. (a) ZnO/BHJ/Fc-Fc^+ before electrical equilibration, (b) PEDOT:PSS/BHJ/BZQ-$BZQ^{\cdot-}$ before electrical equilibration, (c) ZnO/BHJ/Fc-Fc^+ after electrical equilibration, (d) PEDOT:PSS/BHJ/BZQ-$BZQ^{\cdot-}$ after electrical equilibration. In (a) and (c) ZnO acts a selective contact for electrons and Fc-Fc^+ produces a band bending at the BHJ/solution interface enabling the extraction of holes to the solution. In (b) and (d) PEDOT:PSS acts as selective contact for holes and BZQ-$BZQ^{\cdot-}$ induces band bending to extract electrons from the organic layer to the solution.

Conclusions

We have demonstrated that organic photoelectrochemical cells (OPECs) are able to quantitatively extract the photocurrent generated in the organic active layer. The photogenerated charge at the organic active layer is not affected by the presence of the liquid medium. By a careful selection of the redox couple and the interfacial layer, the energetics of the system can be tailored so that the organic blend can provide a flux of either electrons or holes to the solution. Consequently, oxidative or reductive chemistry at the semiconductor/liquid interface can be activated upon demand expanding applicability of the system for the production of different solar fuels. These results can be satisfactorily explained on the basis of the energy diagrams of the devices, which have been constructed with experimental data and Fermi level alignment. The versatility of organic materials is a solid guarantee for further optimization of OPEC devices, which constitute a promising low-cost alternative for the generation of solar fuels.

Methods

Materials

The following materials were used to prepare the OPV and OPEC electrodes: P3HT (Luminescence Technology Corp., MW > 45,000 (GPC)), $PC_{60}BM$ (Solenne, 99.5 %), PEDOT:PSS (CLEVIOS P AI 4083), ZnO (Gene's Ink), MoO_3 (Aldrich, 99.9 %), silver (Aldrich, 99.99 %), ITO (PTB7 labs, 10 Ω/sq), o-dichlorobenzene (Aldrich, 99.9 %).All materials were used as received without further purification. For OPV fabrication, all manipulations were carried out in a glovebox under a nitrogen atmosphere, unless otherwise stated. P3HT:fullerenes blends were prepared from dry o-dichlorobenzene (1:1, 34 mg/ml) and were stirred at 70 °C for16 h before sample preparation. For the preparation of the electrolytic solutions acetonitrile (AlfaAesar, 99.8+%), ferrocene (Aldrich, 98.0 %), benzoquinone (Fluka, 99.5 %), and tetrabutyl hexafluorophosphate

(Fluka, 99.0 %) were used as received without further purification.

Device fabrication

Organic solar cells (OPVs) were fabricated in the configuration ITO/ZnO/P3HT:$PC_{60}BM$/MoO_3/Ag, and 25 mm^2 of active area. Pre-patterned ITO substrates were cleaned and UV-ozone treated. A ZnO nanoparticle solution was spin coated in air at 1000 rpm for 30 seconds followed by thermal treatment at 100 °C for 2 minutes to provide a ZnO layer thickness of ~40 nm. Substrates were transferred to a glovebox equipped with a thermal evaporator and were annealed at 120 °C for 5 minutes. The P3HT:fullerene layer was deposited at speed of 1200 rpm for 30 seconds and was placed in a petri dish to allow slow drying of the film to enable an adequate morphology of the blend. At this point, samples were thermally annealed at 130 °C for 10 min. Evaporation was carried out at a base pressure of 3×10^{-6} mbar to provide different thickness of MoO_3/Ag either 7.5/100 nm (reflective anode) or 7.5/15 nm (semitransparent anode). Devices were encapsulated with a photoresin and a glass microscopy slide. Samples were then taken out of the glovebox for device characterization. Similarly, OPEC electrodes in the configuration ITO/ZnO/P3HT:$PC_{60}BM$ were prepared as above using un-patterned ITO coated glass (4 cm^2) and avoiding the evaporation step. The counter electrode was prepared with chloroplatinic acid, H_2PtCl_6, in ethanol solution onto FTO glass and heating in an oven at 450 ºC for 30 min. A silicon spacer (50 μm thick) was used between the electrode and the counter electrode with a circular hollow space of area 0.26 cm^2 filled with the electrolyte solution. Alternatively, for electrodes replacing ZnO by PEDOT:PSS the spin coating step of PEDOT:PSS was carried out at 5500 rpm for 1 minute, film thickness of ~35 nm.

Device characterization.

Photoelectrochemical characterization was performed in a three-electrode configuration, where a graphite bar and a Ag/Ag^+ ($AgNO_3$ 0.1 M in acetonitrile) were, respectively, used as counterelectrode and as reference. The electrolyte was a 0.1 M tetrabutylammonium hexafluorophosphate solution in acetonitrile with a redox pair ferrocene (Fc/Fc^+,0.16 M) or benzoquinone ($BZQ/BZQ^{\cdot -}$, 0.2 M). The electrodes were illuminated using a 300 W Xe lamp, where the light intensity was adjusted with a thermopile to 100 mW cm^{-2}. All potentials have been referred to the ferrocene redox potential: $E_{Fc/Fc^+} = E_{Ag/Ag^+} - 0.0716$. Capacitance-Voltage measurements were performed with a PGSTAT-30 Autolab potentiostat equipped with a frequency analyzer module, and were recorded by applying a small voltage perturbation (20 mV rms). Measurements were carried out under dark conditions at a frequency of 1000 Hz. External Quantum Efficiency (*EQE*) measurements were performed at short-circuit using a 150 W Xe lamp coupled with a monochromator controlled by a computer. The light intensity was measured using an optical power meter 70310 from Oriel Instruments where a Si photodiode was used to calibrate the system.
Continuous-wave photo-induced absorption spectra were performed in transmission geometry. A 560 nm laser diode served as the pump beam, modulated by a mechanical chopper at a frequency of 133 Hz. Transmission spectra are recorded using a probe beam from a Tungsten halogen lamp, focused on the sample by spherical mirrors in order to avoid chromatic aberrations. The transmitted light is dispersed with a monochromator and detected by a photodiode. The photoinduced variations of the transmission in the sample were recorded using a lock-in amplifier. All the differential spectra have been corrected for the photoluminescence and normalized by the transmission spectrum.

Acknowledgements

We acknowledge the financial support of the European Community through the Future and Emerging Technologies (FET) programme under the FP7, collaborative Project contract nº 309223 (PHOCS). MRA acknowledges contribution thorugh EU project OLIMPIA, FP7-PEOPLE-212-ITN 316832 and by national grant Telethon – Italy, Grant N. GGP12033. We would like to thank Gene's Ink for the supply of ZnO nanoparticles.

Authors contribution

JB conceived the experiments. AG carried out the preparation of all samples and carried out photovoltaic and photoelectrochemical characterization of the devices. MH carried out the photoelectrochemical characterization and CW-PIA measurements. SB prepared the experimental setup and assisted in the CW-PIA measurements. MRA coordinated the CW-PIA experiments, LM designed the experiments and SG and JB coordinated this study. All co-authors discussed the results, AG and MH wrote the first draft of the manuscript, which was revised by all co-authors and the final version was obtained by SG and JB.

Additional information

Supplementary Information accompanies this paper on http://www.nature.com/naturecommunications

Competing financial interests: The authors declare no competing financial interests.

References

1. Fujishima A, Honda K. Electrochemical photolysis of water at a semiconductor electrode. *Nature* **238**, 37-38 (1972).

2. Walter MG, *et al.* Solar Water Splitting Cells. *Chemical Reviews* **110**, 6446-6473 (2010).

3. Ni M, Leung MKH, Leung DYC, Sumathy K. A review and recent developments in photocatalytic water-splitting using TiO2 for hydrogen production. *Renewable & Sustainable Energy Reviews* **11**, 401-425 (2007).

4. Hamann TW. Splitting water with rust: hematite photoelectrochemistry. *Dalton Transactions* **41**, 7830-7834 (2012).

5. Tacca A, *et al.* Photoanodes Based on Nanostructured WO3 for Water Splitting. *Chemphyschem* **13**, 3025-3034 (2012).

6. Park Y, McDonald KJ, Choi KS. Progress in bismuth vanadate photoanodes for use in solar water oxidation. *Chemical Society Reviews* **42**, 2321-2337 (2013).

7. Prévot MS, Sivula K. Photoelectrochemical Tandem Cells for Solar Water Splitting. *The Journal of Physical Chemistry C* **117**, 17879-17893 (2013).

8. Sariciftci NS, Smilowitz L, Heeger AJ, Wudl F. Photoinduced Electron Transfer from a Conducting Polymer to Buckminsterfullerene. *Science* **258**, 1474-1476 (1992).

9. Green MA, Emery K, Hishikawa Y, Warta W, Dunlop ED. Solar cell efficiency tables (version 39). *Prog Photovoltaics* **20**, 12-20 (2012).

10. He Z, Zhong C, Su S, Xu M, Wu H, Cao Y. Enhanced power-conversion efficiency in polymer solar cells using an inverted device structure. *Nature Photonics* **6**, 591-595 (2012).

11. Danziger J, Dodelet JP, Armstrong NR. Electrochemical and photoelectrochemical processes on thin films of perylenetetracarboxylic dianhydride. *Chemistry of Materials* **3**, 812-820 (1991).

12. Gautam V, Bag M, Narayan KS. Dynamics of Bulk Polymer Heterostructure/Electrolyte Devices. *The Journal of Physical Chemistry Letters* **1**, 3277-3282 (2010).

13. Janaky C, de Tacconi NR, Chanmanee W, Rajeshwar K. Electrodeposited Polyaniline in a Nanoporous WO3 Matrix: An Organic/Inorganic Hybrid Exhibiting Both p- and n-Type Photoelectrochemical Activity. *Journal of Physical Chemistry C* **116**, 4234-4242 (2012).

14. Lanzarini E, *et al.* Polymer-Based Photocatalytic Hydrogen Generation. *The Journal of Physical Chemistry C* **116**, 10944-10949 (2012).

15. Suppes G, Ballard E, Holdcroft S. Aqueous photocathode activity of regioregular poly(3-hexylthiophene). *Polymer Chemistry* **4**, 5345-5350 (2013).

16. Wang ZF, *et al.* Polypyrrole sensitized ZnO nanorod arrays for efficient photo-electrochemical splitting of water. *Physica B-Condensed Matter* **419**, 51-56 (2013).

17. Yohannes T, Solomon T, Inganas O. Polymer-electrolyte-based photoelectrochemical solar energy conversion with poly(3-methylthiophene) photoactive electrode. *Synthetic Metals* **82**, 215-220 (1996).

18. Gazotti WA, Nogueira AF, Girotto EM, Gallazzi MC, De Paoli MA. Flexible photoelectrochemical devices based on conducting polymers. *Synthetic Metals* **108**, 151-157 (2000).

19. Sergawie A, Yohannes T, Günes S, Neugebauer H, Sariciftci NS. Photoelectrochemical Cells based on Emeraldine Base Form of Polyaniline. *J Braz Chem Soc* **18**, 1189-1193 (2007).

20. Boix PP, Guerrero A, Marchesi LF, Garcia-Belmonte G, Bisquert J. Current-Voltage Characteristics of Bulk Heterojunction Organic Solar Cells: Connection Between Light and Dark Curves. *Advanced Energy Materials* **1**, 1073-1078 (2011).

21. Boix PP, Garcia-Belmonte G, Munecas U, Neophytou M, Waldauf C, Pacios R. Determination of gap defect states in organic bulk heterojunction solar cells from

capacitance measurements. *Applied Physics Letters* **95**, 233302 (2009).

22. Dibb GFA, *et al.* Influence of doping on charge carrier collection in normal and inverted geometry polymer:fullerene solar cells. *Sci Rep* **3**, (2013).

23. Guerrero A, *et al.* How the Charge-Neutrality Level of Interface States Controls Energy Level Alignment in Cathode Contacts of Organic Bulk-Heterojunction Solar Cells. *ACS Nano* **6**, 3453-3460 (2012).

24. Osterloh FE, Holmes MA, Chang LL, Moule AJ, Zhao J. Photochemical Charge Separation in Poly(3-hexylthiophene) (P3HT) Films Observed with Surface Photovoltage Spectroscopy. *Journal of Physical Chemistry C* **117**, 26905-26913 (2013).

25. Mora-Sero I, *et al.* Selective contacts drive charge extraction in quantum dot solids via asymmetry in carrier transfer kinetics. *Nat Commun* **4**, (2013).

26. Marcus RA. On the Theory of Oxidation-Reduction Reactions Involving Electron Transfer. I. *The Journal of Chemical Physics* **24**, 966-978 (1956).

27. Marcus RA. Electron transfer reactions in chemistry. Theory and experiment. *Reviews of Modern Physics* **65**, 599-610 (1993).

28. Österbacka R, An CP, Jiang XM, Vardeny ZV. Two-Dimensional Electronic Excitations in Self-Assembled Conjugated Polymer Nanocrystals. *Science* **287**, 839-842 (2000).

29. Antognazza MR, Ghezzi D, Musitelli D, Garbugli M, Lanzani G. A hybrid solid-liquid polymer photodiode for the bioenvironment. *Applied Physics Letters* **94**, - (2009).

30. Noone KM, Subramaniyan S, Zhang Q, Cao G, Jenekhe SA, Ginger DS. Photoinduced Charge Transfer and Polaron Dynamics in Polymer and Hybrid Photovoltaic Thin Films: Organic vs Inorganic Acceptors. *The Journal of Physical Chemistry C* **115**, 24403-24410 (2011).

31. Noone KM, Strein E, Anderson NC, Wu P-T, Jenekhe SA, Ginger DS. Broadband Absorbing Bulk Heterojunction Photovoltaics Using Low-Bandgap Solution-Processed Quantum Dots. *Nano Letters* **10**, 2635-2639 (2010).

32. Chin XY, Yin J, Wang Z, Caironi M, Soci C. Mapping polarons in polymer FETs by charge modulation microscopy in the mid-infrared. *Sci Rep* **4**, (2014).

33. Fabregat-Santiago F, Garcia-Belmonte G, Mora-Sero I, Bisquert J. Characterization of nanostructured hybrid and organic solar cells by impedance spectroscopy. *Phys Chem Chem Phys* **13**, 9083-9118 (2011).

34. Ghezzi D, *et al.* A polymer optoelectronic interface restores light sensitivity in blind rat retinas. *Nature Photonics* **7**, 400-406 (2013).

35. Ripolles TS, Guerrero A, Garcia-Belmonte G. Polymer defect states modulate open-circuit voltage in bulk-heterojunction solar cells. *Applied Physics Letters* **103**, - (2013).

36. Nardes AM, Kemerink M, de Kok MM, Vinken E, Maturova K, Janssen RAJ. Conductivity, work function, and environmental stability of PEDOT : PSS thin films treated with sorbitol. *Organic Electronics* **9**, 727-734 (2008).

37. Jiang X, Wong FL, Fung MK, Lee ST. Aluminum-doped zinc oxide films as transparent conductive electrode for organic light-emitting devices. *Applied Physics Letters* **83**, 1875-1877 (2003).

38. Bard AJ, Stratmann M, Licht S. Encyclopedia of Electrochemistry, Volume 6, Semiconductor Electrodes and Photoelectrochemistry. In: *Encyclopedia of Electrochemistry* (ed^(eds). Wiley-VCH (2002).